Supplementary Information

Synergistic Effect of Hydrogen-Bond Interaction and Interface Regulation for Stable Aqueous Sodium-Ion Batteries

Lingyu Du, Miaomiao Xie, Zizhen Liu, Weiyu Cao, Jianchao Sun, and Litao Kang**

L. Y. Du, M. M. Xie, Z. Zh. Liu, W. Y. Cao, J. C. Sun, L. T. Kang
School of Environmental and Material Engineering, Yantai University, Yantai, 264005, P. R. China
E-mail: dulingyu91@163.com; kanglitao@ytu.edu.cn

Experimental Section

Material Synthesis:

NaFeMnPBAs was synthesized by co-precipitation method. Typically, 2.0 mmol of $K_4Fe(CN)_6·3H_2O$ was dissolved in 100 mL of saturated NaCl solution, which was denoted as A. 1.3 mmol of $MnSO_4·H_2O$ and 0.7 mmol of $FeSO_4·7H_2O$ were dissolved in 80 mL of saturated NaCl solution, which was denoted as B. Then, the B solution was slowly dropped into the A solution under magnetic stirring. After that, the reaction was maintained at 60 °C for 12 h. When the temperature was cooling down, the NaFeMnPBAs powder was obtained through centrifugation and drying.

NTP/CNTs was synthesized by the solvothermal method. The CNTs were pre-treated by the HNO_3 according to the previously literature. Typically, 100 mg CNTs were dispersed into 40 mL of ethanol under ultrasonication and magnetic stirring. Then, 2.0 mmol titanium (IV) butoxide was added into the above mixture, which was denoted as A. 2.0 mmol CH_3COONa was dissolved into 6 mL of phosphorous acid solution (85 wt%), which was denoted as B. A and B solutions were mixed uniformly under magnetic stirring. Then it was transferred into Teflon-lined stainless-steel autoclave and heated in an oven at 160 °C for 3 h. Finally, the NTP/CNTs was obtained after filtration and drying.

Electrolyte Preparation: The hybrid electrolyte was prepared by mixing $NaCF_3SO_3$ and DOL, urea, deionized water. The concentration of $NaCF_3SO_3$ is 4 m (mol kg^{-1}). The molar ratio of DOL, urea and deionized water is 1.5:0.5:1. For comparison, conventional aqueous electrolyte, DOL/H_2O and urea/H_2O-based electrolytes were also prepared with the same ratios in the hybrid electrolyte.

Electrode Preparation: The NaFeMnPBAs electrodes were prepared by mixing active materils, cabon black (CABOT BP 2000), and polyvinylidene difluoride with a weight ratio of 7:2:1 in N-methyl-2-pyrrolidone and then coating the slurry on carbon cloth. The areal mass loading of NaFeMnPBAs on the carbon cloth was 2-3 mg cm^{-2}. The NTP/CNTs electrodes were prepared via the above mentioned method with an areal mass loading of 2-3 mg cm^{-2}. In addition, the activated carbon electrodes were fabricated by mixing activated carbon, acetylene black and polyvinylidene difluoride with a mass ratio of 8:1:1 in N-methyl-2-pyrrolidone and then coating the slurry on carbon cloth. The areal mass loading of activated carbon was ~15 mg cm^{-2}. The size of above electrodes is 0.785 cm^{-2}.

Electrochemical Measurement: The voltage window of $NaCF_3SO_3$ electrolytes was measured by linear sweep voltammetry (LSV) in a three-electrode cell, in which Ti foil, Ag/AgCl (saturated KCl solution) and Pt foil were used as working electrode, reference electrode and counter electrode, respectively. A three-electrode Swagelok cell and coin cell were used to test the electrochemical properties of NaFeMnPBAs electrodes and the full cells, respectively. The mass ratio of cathode to anode was ~1:1.

Linear sweep voltammetry (LSV) and cyclic voltammetry (CV) tests were carried out on an electrochemical workstation (CHI Instruments, CHI660E). The galvanostatic discharge/charge (GCD) measurements were conducted on the battery test systems (NEWARE, CT2001A). The galvanostatic intermittent titration technique (GITT) measurement was performed on the battery test system (LAND, CT2001A) with the test profile of discharging at 0.1 A g^{-1} for 1 min and rest for 60 min. The electrochemical impedance spectra (EIS) was measured in the frequency range of 100 kHz-10 mHz (for battery) and 100 kHz-1 Hz (for electrolyte) with an AC voltage amplitude of 5 mV.

Characterization: The morphology was characterized by transmission electron microscopy (TEM, TF20) and scanning electron microscopy (SEM, TESCAN MIRA LMS). The structure was characterized by XRD (Rigaku Ultima IV) with a Cu Kα wave. XPS spectra were collected through Thermo Scientific K-Alpha spectrometer using an Al Kα source, and binding energies were calibrated using carbon (C 1s=284.8 eV). FTIR spectra were collected on Thermo Scientific Nicolet iS20 and INVENIO S. The Raman spectra were collected on Horiba LabRAM HR Evolution with 532 nm laser. The ^{1}H NMR spectra were acquired on a Bruker Ascend spectrometer using 500 MHz. The dissolution amount of Mn and Fe in the electrolyte was measured by inductively coupled plasma-atomic emission spectrometry (ICP-OES, Thermo Fisher iCAP PRO).

Computational Methods: Quantum chemistry calculations were first performed to optimize DOL, urea, $NaCF_3SO_3$ molecular geometries of additives molecule using the Gaussian 16 package at B3LYP/6-311+G(d) level of theory. The atomistic force field parameters for all ions and molecules are described by the OPLS-AA. The SPC/E water model was adopted in the current work. Atomistic simulations were performed using GROMACS package with cubic periodic boundary conditions. The equations for the motion of all atoms were integrated using a classic Verlet leapfrog integration algorithm with a time step of 2.0 fs. A cutoff radius of 1.0 nm was set for short-range van der Waals interactions and real-space electrostatic interactions. The particle-mesh Ewald (PME) summation method with an interpolation order of 4 and a Fourier grid spacing of 0.12 nm was employed to handle long range electrostatic interactions in reciprocal space. In all the three directions, periodic boundary conditions were imposed. Leapfrog algorithm was used to integrate the Newtonian equation of motion. The MD simulation was processed in an NPT ensemble and the simulation time is 20 ns. In NPT simulations, the pressure was maintained at 1 bar by the Berendsen barostat in an isotropic manner and the temperature was maintained by the V-rescale thermostat at 298.15 K.

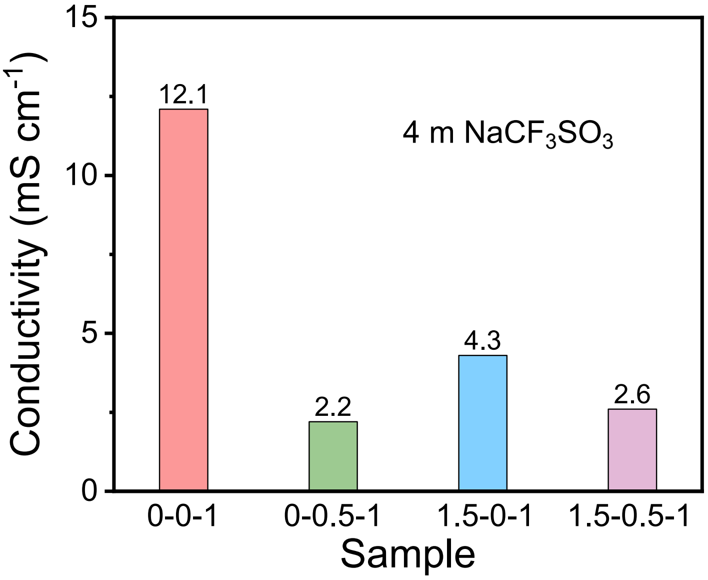

Fig. S1 Ionic conductivity of the electrolytes.

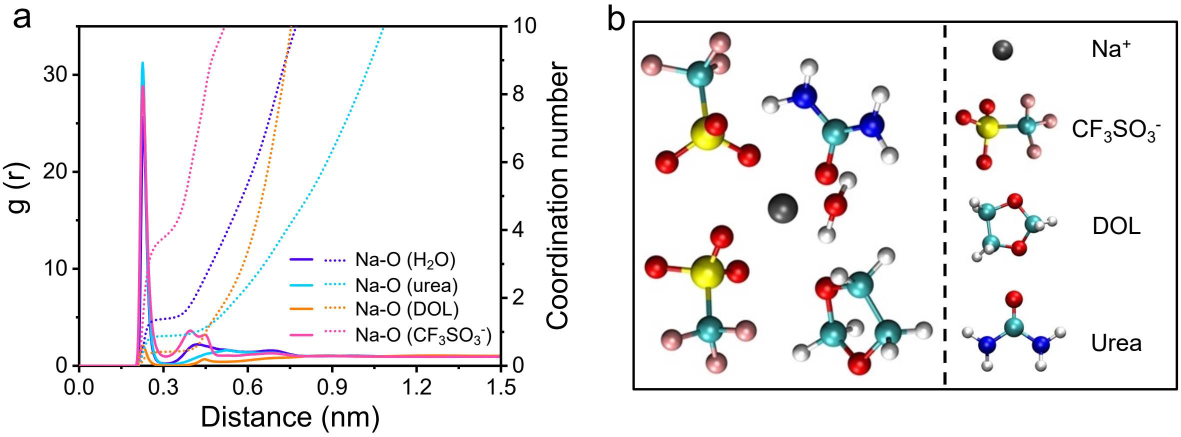

Fig. S2 (a) RDF plots of Na-O (H_2O), Na-O (DOL), Na-O (urea) and Na-O ($CF_3SO_3^-$), and the corresponding average coordination number of 1.5-0.5-1 electrolyte. (b) MD simulation snapshots.

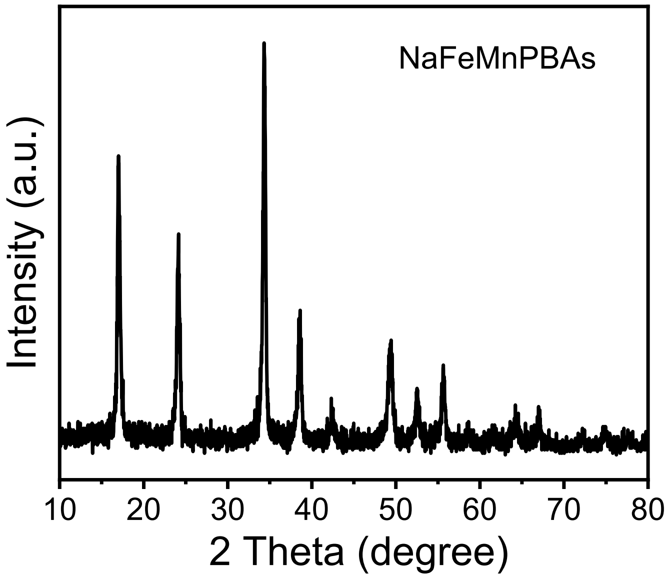

Fig. S3 XRD pattern of the NaFeMnPBAs.

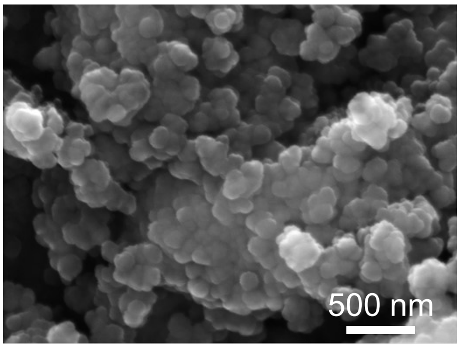

Fig. S4 SEM images of NaFeMnPBAs.

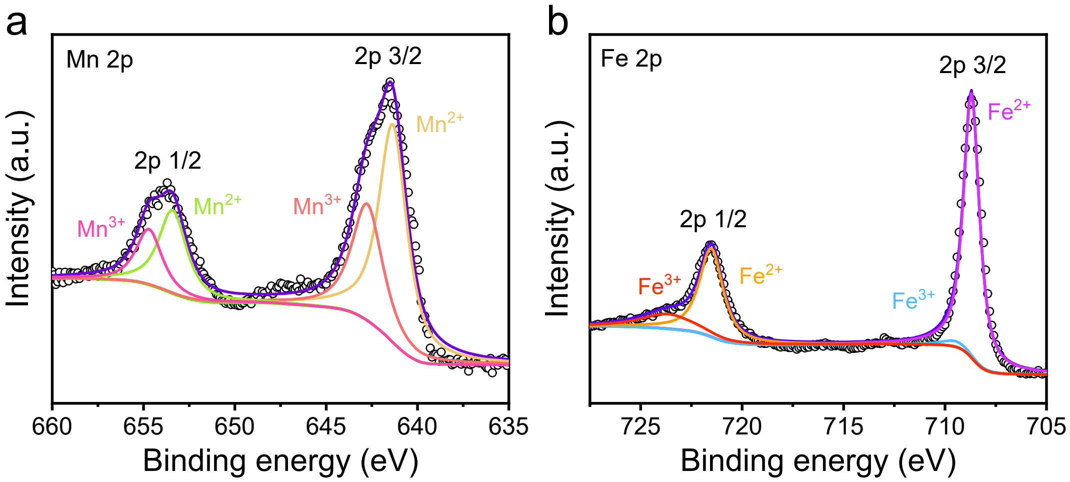

Fig. S5 (a) Mn 2p, (b) Fe 2p XPS spectra of NaFeMnPBAs.

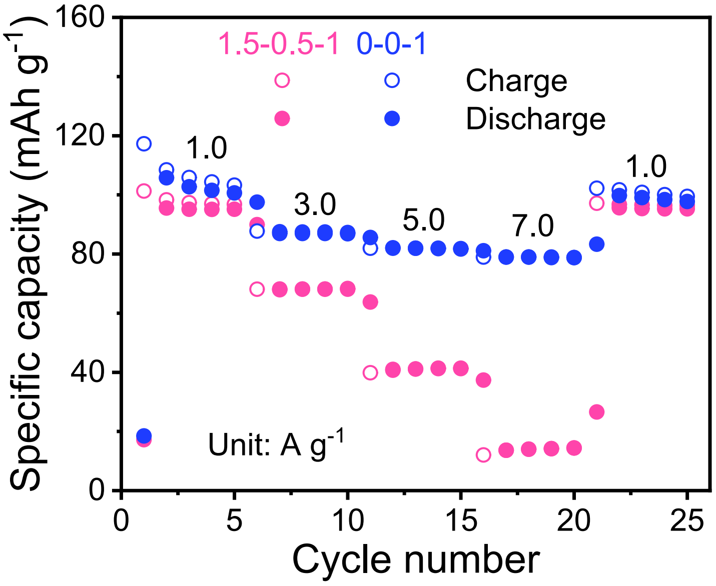

Fig. S6 (a) Rate performance of NaFeMnPBAs electrodes in 0-0-1 and 1.5-0.5-1 electrolytes.

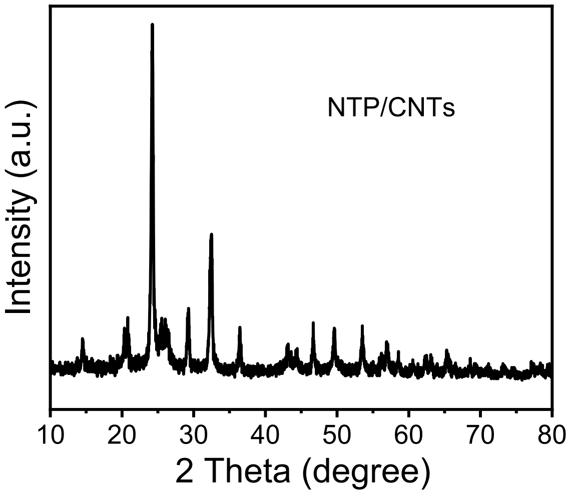

Fig. S7 XRD pattern of NTP/CNTs.

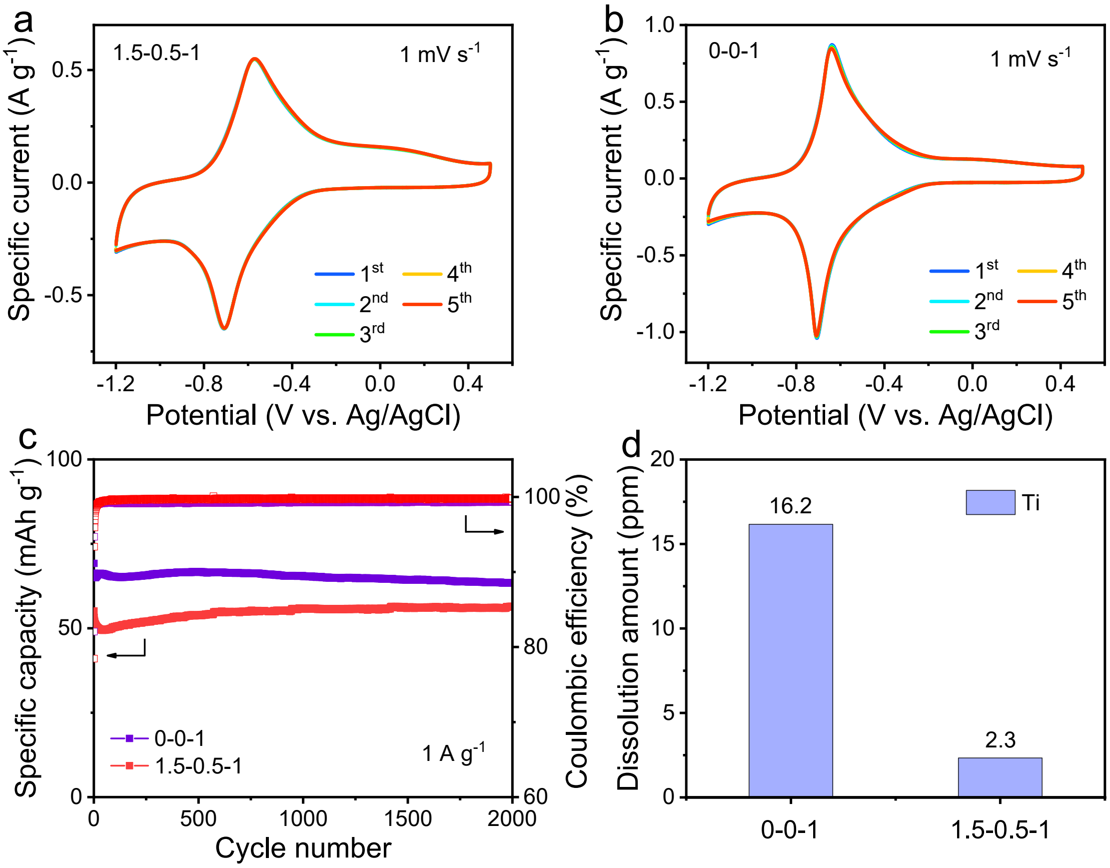

Fig. S8 Electrochemical performances of NTP/CNTs electrodes in 0-0-1 and 1.5-0.5-1 electrolytes. (a,b) CV curves at 1 mV s^{-1}. (b) Cycling performance at 1 A g^{-1}. (c) Dissolution amount of Ti element of NTP/CNTs in electrolyte.

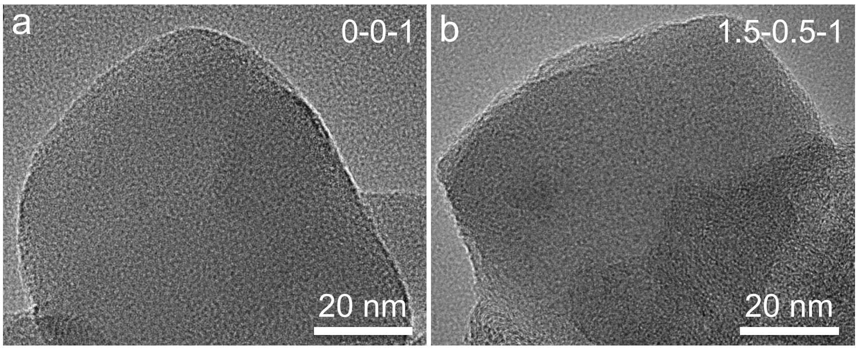

Fig. S9 HRTEM images of NaFeMnPBAs after cycling in (a) 0-0-1 and (b) 1.5-0.5-1 electrolytes.

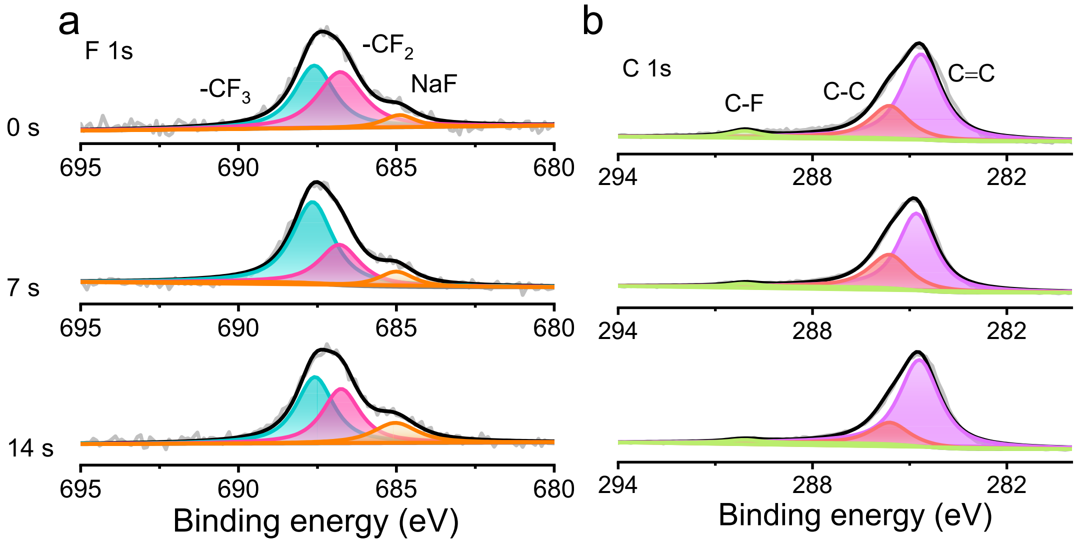

Fig. S10 XPS spectra of NaFeMnPBAs electrode cycling at 0-0-1 electrolyte under Ar^+ sputtering at 0 s, 7 s, and 14 s. (a) F 1s, (b) C 1s.

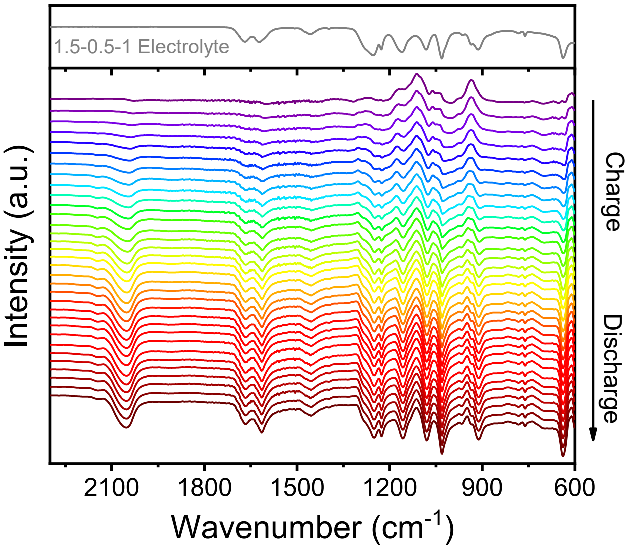

Fig. S11 In situ FTIR spectra of NaFeMnPBAs electrode during charging and discharging process.

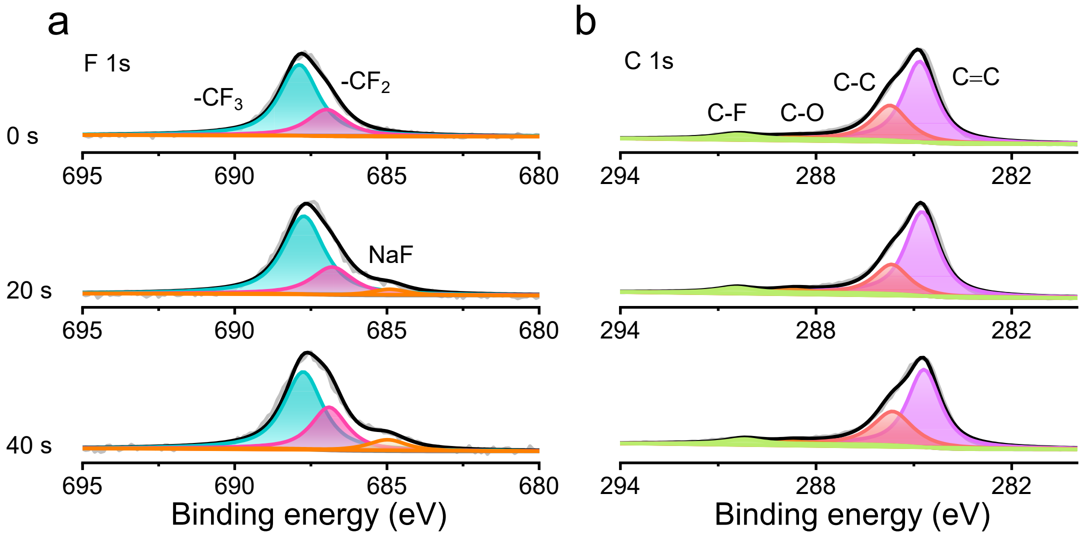

Fig. S12 XPS spectra of NTP/CNTs electrode cycling at 1.5-0.5-1 electrolyte under Ar^+ sputtering at 0 s, 7 s, and 14 s. (a) F 1s, (b) C 1s.

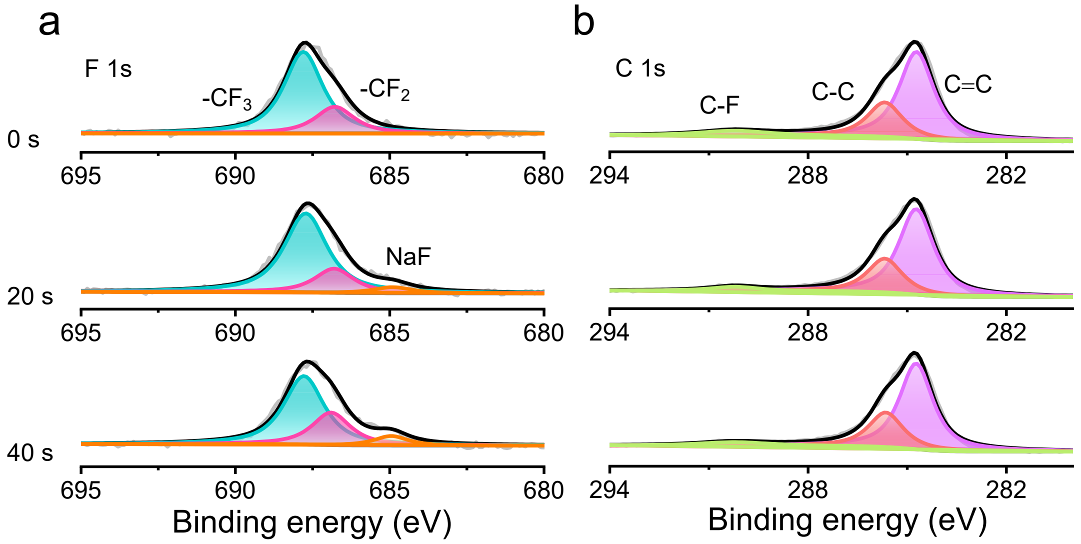

Fig. S13 XPS spectra of NTP/CNTs electrode cycling at 0-0-1 electrolyte under Ar$^+$ sputtering at 0 s, 7 s, and 14 s. (a) F 1s, (b) C 1s.

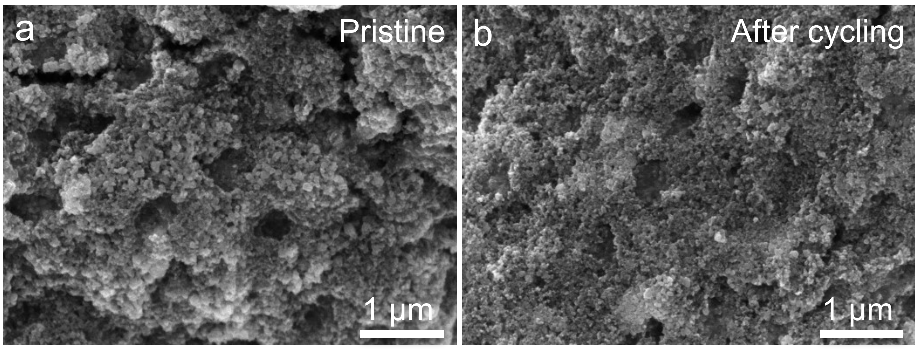

Fig. S14 SEM images of NaFeMnPBAs electrodes (a) before and (b) after cycling in 1.5-0.5-1 electrolyte.

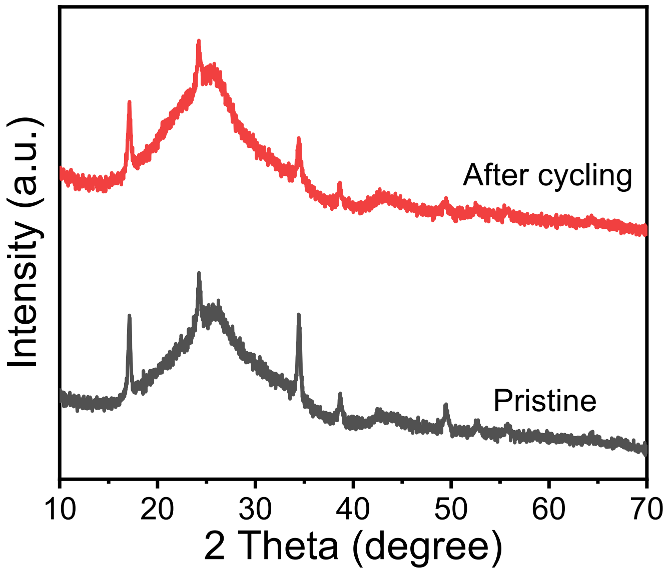

Fig. S15 XRD patterns of NaFeMnPBAs electrodes before and after cycling in 1.5-0.5-1 electrolyte.